

Outage probability of SSTS for distributed antenna systems over Rayleigh fading channels in multi-cell environment

Sitong Lv^{1,2} · Zhihong Qian¹ · Yuxi Liu³

Received: 3 July 2017 / Revised: 30 September 2017 / Accepted: 7 October 2017 / Published online: 20 October 2017
© Springer Science+Business Media, LLC 2017

Abstract In this paper, downlink outage probability for distributed antenna systems (DAS) in multicell environment is proposed, while based on maximum desired signal criterion, a single selection transmission scheme (SSTS) is proposed. Usually, adopting central limit theorem (CLT) method, the component of interference plus noise is considered as a fixed-variance Gaussian random variable in most papers. However, the aforementioned method does not reflect the effect of short-term fading on interference and its usage is in the constraints of restrictive conditions. To relax the constraints, non-central limit theorem (NCLT) is introduced, which treats the variance of interference plus noise as a changeable-variance random variable influenced by short-term fading. It is assumed that channels are independent identical Rayleigh fading with propagation path-loss, and the closed-form expression of outage probability for DAS is derived. Finally, simulation results demonstrate the validity of theoretical analysis.

Keywords Distributed antenna systems · Outage probability · Single selection transmission scheme (SSTS) · Non-central limit theorem

1 Introduction

In wireless communications, the conflict between the continuous improved quality of experience (QoE) and the lagged

performance of current cellular networks becomes more and more obvious. This is because the improved QoE requires much higher data rates for support, which can be realized by more available spectrum resource. However, the spectrum resource utilized by cellular networks constrained is more and more precious, and there are no additional spectrum resources assigned to cellular networks. Distributed antenna systems (DAS) has been introduced as a key technology for next generation communications for expanding coverage and increasing sum rates. Different from a conventional antenna system (CAS) which has centralized antennas at the center location, in DAS, distributed antenna (DA) ports which are physically connected with each other via dedicated channels are separated geographically throughout a cell. Therefore, the access distance for each user along with the transmit power and co-channel interference can be reduced in DAS, which results in improved overall performance [1]. Recently, the distributed antenna system (DAS) has been regarded as a promising technique for the design of future network architectures, since it has great potential for capacity improvement and coverage extension [2,3]. It also meets the increasing demand for high spectral efficiency and good coverage [4–6]. Distributed antenna systems (DAS) as a feasible technology are first proposed and adopted to cover any dead spots in indoor wireless communications [7]. However, the application scope of DAS has been expanded to other domains, such as better coverage, increased battery life, as well as improved signal-to-interference plus noise (SINR) at receiver [8].

An overview of distributed wireless communication systems (DWCS) and the corresponding advantages for it were described in [9]. Similar to DWCS, the configuration of remote antenna units (RAUs) in DAS is geographically distributed, in order to bridge the distance between transmitter and receiver, which can improve communication quality [10], while the antenna units within conventional co-located

✉ Sitong Lv
lihailin830128@163.com

¹ Jilin University, Changchun, China

² Aviation University of AirForce, Jilin, China

³ State Grid Information and Telecommunication Group Co., Ltd., Beijing, China

antenna systems (CAS) are centralised at a fixed location. In DAS, a central processing unit (CPU) is configured to provide high speed and reliable data transmission for each cell. The communication channels between CPU and RAUs are realized through optical fibre, exclusive frequency link, and so on. According to the configuration of DAS, it is considered to be cooperative communications, as a recently developed technique in the next few years [11, 12].

Adopting the central limit theorem (CLT) method, the system performance of DAS has been analyzed for the most existing works [8, 10, 13, 14]. For the CLT method, interference plus noise of communications is assumed as fixed-variance Gaussian noise, when propagation path-loss and transmitted power are given. In other words, the interference power of communication for DAS is treated as a constant. The disadvantages of CLT method in DAS is that the role of short-term fading on interference cannot be employed. The precondition for CLT method is that the number of interference and noise items is sufficient, but in most cases this condition is not satisfied. If interference plus noise terms are sparse, the analytical result does output an error, and it should not be neglected. Therefore, we propose a non-central limit theorem (NCLT) method to overcome the aforementioned limitations in this paper. Compared with CLT method, the interference power as well as the variance of it in DAS are treated as random variable simultaneously for the proposed NCLT method. For NCLT method, the effect of short-term fading on the variance of interference power can be shown, while the CLT method is not. So NCLT method can evaluate the system performance more practically and accurately in comparison with the CLT method. For NCLT method, many scholars have conducted a lot of researches. Channels between CPU and RAUs assumed to suffer from Rayleigh fading, the capacity, bit error rate (BER) and outage probability for blanket transmission scheme (BTS, i.e., all of the RAUs within cell broadcast data) in DAS have been studied [15]. While Choi et al. have done research on the capacity of DAS with Gaussian fading for channels between mobile terminals (MTs) and RAUs [16].

Another challenge for future information and communication (ICT) technologies is to reduce the power consumption. Against power-saving, Vereecken et al. [17] introduced sleep modes for communication nodes. On the basis of maximum desired signal criterion, a single selection transmission scheme (SSTS) is proposed to reduce energy, in which one of the RAUs is chosen for transmission and the rest of RAUs are sleeping. As far as we know, the studies of system performance of DAS for SSTS are few. Adopting CLT method, we have analyze the capacity and outage probability of DAS for SSTS, where the interference plus noise is regarded as fixed-variance Gaussian noise [18]. Adopted NCLT method, the BER for SSTS has been analyzed in [19]. However, the studies of the outage probability for SSTS does not, hence

we do research on outage probability for SSTS with NCLT method.

In this paper, the main contributions are summarized as follows: (1) the interference power as well as its variance in DAS are treated as random variable simultaneously. The effect of short-term fading on the corresponding variance is embodied. So this NCLT method is more practical and accurate to evaluate the system performance of DAS. (2) An SSTS strategy is proposed on the basis of maximum desired signal criterion. Downlink outage probability of DAS for the proposed SSTS is investigated and the closed-form expressions of it are derived under no shadowing conditions, while the corresponding approximate analytical expressions for shadowing conditions are also given.

The rest of paper is organized as follows: the DAS model is described in Sect. 2. The outage probability of SSTS for DAS is derived in Sect. 3. Section 4 discusses some practical concerns, and provides numerical results together with some discussions. Finally, the key conclusions from this research are summarised in Sect. 5.

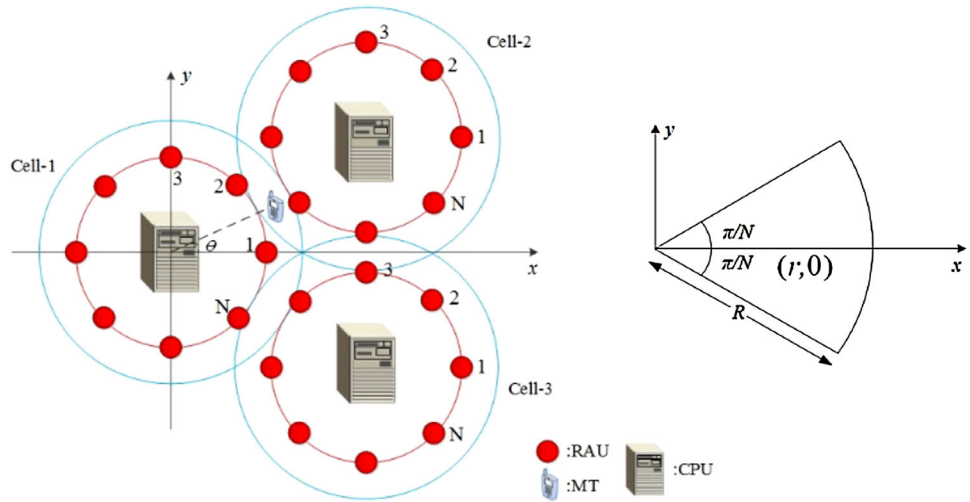
Notation: scalar, vectors, and matrices are represented by lowercase plain-font letters, lowercase bold-font letters, and uppercase bold-font letters throughout the paper, respectively. $(\cdot)^H$ and $E_h[\cdot]$ denote the conjugate transpose matrix and the expectation to h , respectively. $f_X(x)$ represents the probability density function (PDF) against random variable X . $\ln(\cdot)$ and $\log_{10}(\cdot)$ are the nature logarithm and common logarithm, respectively.

2 System and channel model

In each reference cell, a CPU located in a fixed position is configured in DAS. The communication channels between CPU and the RAUs in the corresponding cell are connected via dedicated wire. However, the CPUs from different cell are independent with each other. As shown in Fig. 1, the Wyner's planar cellular deployment is introduced in this paper [14, 20]. For Wyner model, arbitrarily cell can receive the signal from the two adjacent cells, which is referred to as inter-cell interference. In actual deployment, coverage, user number as well as other environmental factors are taken into consideration for the RAUs number of each cell [21].

In cellular system, each cell coverage in DAS is usually circular, and the RAUs in the corresponding cell are located on a red circle, which is called circular layout (CL) [22, 23]. Therefore, the coverage of cell is expressed by a circle with radius R , while the radius of another circle RAUs located on and uniformly distributed, is r . As shown in Fig. 1, the number of RAUs within each cell is N , and its corresponding coverage region is represented by solid lines. The coverage region of RAUs is congruent sector, and the central angles for that of it is $2\pi/N$, as depicted in Fig. 1 [24]. Each RAU in the cell is located on the bisector of the central angle.

Fig. 1 Configuration of a distributed antenna system



The following hypotheses are made for this paper:

- All of the RAUs and mobile terminals (MTs) support one omni-directional antenna. MT located in Cell i is designated as MT_i , while the index of RAUs within each cell is labeled by RAU_j , and the angle between objective cell centre, MT, and the horizontal is denoted as theta as depicted in Fig. 1.
- Within each cell, only one MT is active, which can be realised by adopting time-division multiple access (TDMA) techniques. Moreover, the channels between MTs and RAUs suffer from block fading, i.e. the fading coefficients for channels keep unchanged within a packet interval and vary among different packets.

2.1 Linear Wyner architecture

Arbitrary one cell is chosen as the object of study and denoted as Cell 1. The corresponding two adjacent cells around Cell 1 are labeled as Cell 2 and Cell 3 respectively. The transmitted power for the i th RAU in the j th cell is written as $P_i, j(i = 1, \dots, N; j = 1, 2, 3)$; as a consequence, the total transmitted power of each cell in DAS is the same, i.e., $P = \sum_{i=1}^N P_{i,j}$.

For the j th cell, the distances between MT and RAUs are written as $d_{i,j}$, and the corresponding propagation path-loss is written as $L_{i,j} = K d_{i,j}^{-\alpha}$, where α is the path-loss exponent, K is a unitless constant depending on antenna characteristics and average channel attenuation. From the perspective of simplicity, we set $K = 1$.

2.2 Channel model and received signal

For each cell in DAS, all of the distributed antennas (DAs) broadcast signal to the corresponding active MT with blanket transmission scheme (BTS), and vice versa. In objective cell,

the discrete time-base band signal received at MT for BTS is written as:

$$y = \sqrt{S_s} \mathbf{h}^{(1)} \mathbf{x}^{(1)} + \sqrt{S_s} \sum_{j=2,3} \mathbf{h}^{(j)} \mathbf{x}^{(j)} + n \tag{1}$$

where

$\mathbf{h}^{(j)} = [\sqrt{S_s} h_{1,j}, \dots, \sqrt{S_s} h_{N,j}]$ denote channel vector in the j th cell, $h_{i,j}$ is the short-term fading between the active MT in the j th cell and the i th RAU in the corresponding cell, and it is assumed to suffer from independent identical Rayleigh fading. While $L_{i,j}$ denotes the corresponding propagation path-loss.

$\mathbf{x}^{(j)} = [x_{1,j}, \dots, x_{N,j}]^T$ is the transmitted signal vector from all of the RAUs in the j th cell, $x_{i,j}$ is the corresponding transmitted signal from the i th RAU, and the average power for that of it is $E [|x_{i,j}|^2] = P_{i,j}$.

n is the additive Gaussian noise with variance $E [nn^H] = \sigma_n^2$, which is assumed to be independent of signal $x_{1,j}$.

Here, s characterises the shadowing effect, whose probability density function (PDF) is expressed as log-normal distribution [25]:

$$f_{S_s}(s) = \frac{\xi}{\sqrt{2\pi}\sigma_s} \exp \left[-\frac{(10 \lg s - \mu)^2}{2\sigma^2} \right] \tag{2}$$

where $\xi = 10/(\ln 10)$, μ (in dB) and σ (in dB) denote the mean and standard deviation for $10 \log_{10} s$, respectively. Meanwhile, from the perspective of simplicity, the channels between RAUs and MTs are assumed to be independent identically distributed shadow fading. According to the aforementioned equation, it can be derived that $S = 1$ is the means of no shadowing.

3 Closed-form of outage probability for STSS

In the following section, we will derive the closed-form expressions of outage probability for shadowing scenarios as well as the corresponding approximate expressions for shadowing case under downlink cellular DAS environment. It is assumed that the channel state information can be obtained at the receiver.

The proposed SSTS method in this paper is on the basis of the maximum desired signal criterion. For this selection scheme, the channel with feature of the largest signal intensity is selected to transmit signal, while the remainder of channels in the objective cell is sleep to save energy. Moreover, the selection of channel between active MT and RAUs from adjacent cells (Cell j , $j = 2, 3$) is random. In this case, the received signal at the active MT is given by:

$$y_1 = \underbrace{\sqrt{S_s L_{k,1}} h_{k,1} x_{k,1}}_{\text{desired signal}} + \underbrace{\sqrt{S_s L_{q,2}} h_{q,2} x_{q,2} + \sqrt{S_s L_{l,3}} h_{l,3} x_{l,3}}_{\text{interference}} + n_{\text{noise}} \quad (3)$$

where $k = \arg \max_{i \in \{1, \dots, N\}} \{z_{i,1}\}$, q and l are randomly selected from $D = \{1, \dots, N\}$, respectively.

According to Eq. (3), the signal to interference plus noise ratio (SINR) at the MT in objective cell is written as:

$$\gamma = \frac{L_{k,1} P_{k,1} |h_{k,1}|^2}{L_{q,2} P_{q,2} |h_{q,2}|^2 + L_{l,3} P_{l,3} |h_{l,3}|^2 + \sigma_n^2 / S_s} \quad (4)$$

The interference plus noise and its variance are treated as random variable simultaneously, which is different from the most existing works adopted CLT method. For CLT method, the variance is considered as constant rather than a random variable.

Since $h_{i,j}$ follows the Rayleigh distribution, the PDF of $|h_{i,j}|^2 L_{i,j} P_{i,j}$ is an exponential distribution with mean value $L_{i,j} P_{i,j}$.

The received desired signal at MT from all of the RAUs within Cell 1 are denoted by $Z = \{z_{1,1}, \dots, z_{N,1}\}$, where $z_{i,1} = |h_{i,1}|^2 L_{i,1} P_{i,1}$. The expected values of the elements in Z are re-denoted as $\Omega = \{\bar{z}_1, \dots, \bar{z}_{|D|}\}$, in which $|D|$ is the cardinality of D . Let $z_{\max} = \max_{i \in \{1, \dots, N\}} \{z_{i,1}\}$, so Eq. (4) can be rewritten as:

$$\gamma = \frac{z_{\max}}{L_{q,2} P_{q,2} |h_{q,2}|^2 + L_{l,3} P_{l,3} |h_{l,3}|^2 + \sigma_n^2 / S_s} \quad (5)$$

The maximum desired signal can be indexed by $z_{\max} = \max_{i \in \{1, \dots, N\}} \{z_{i,1}\}$, and its corresponding PDF can be derived and given as [14]:

$$f_{z_{\max}}(z) = \frac{d}{dz} \left[\prod_{i=\{1, \dots, |D|\}} \left(1 - \exp\left(-\frac{z}{\bar{z}_i}\right) \right) \right] \quad (6)$$

Let Ω_{vu} denote the v th u -subset of the set Ω , i.e., the v th subset of Ω which includes exactly u elements ($u = 1, \dots, |D|$, $v = 1, \dots, \binom{|D|}{u}$). The elements from Ω are denoted by $\eta_{u,v,w}$ ($w = 1, \dots, u$). In consideration of the relationship between \bar{z}_i and $\eta_{u,v,w}$, the product in Eq. (6) can be expanded with the proposed method in [26]:

$$\begin{aligned} & \prod_{i \in D} \left(1 - \exp\left(-\frac{z}{\bar{z}_i}\right) \right) \\ &= 1 - \sum_{u=1}^{|D|} (-1)^{u-1} \sum_{v=1}^{\binom{|D|}{u}} \prod_{w=1}^u \exp\left(-\frac{z}{\eta_{u,v,w}}\right) \\ &= 1 - \sum_{u=1}^{|D|} (-1)^{u-1} \sum_{v=1}^{\binom{|D|}{u}} \exp\left(-z \sum_{v=1}^u \eta_{u,v,w}\right) \\ &= 1 - \sum_{u=1}^{|D|} (-1)^{u-1} \sum_{v=1}^{\binom{|D|}{u}} \exp(-\lambda_{uv} z) \end{aligned} \quad (7)$$

According to the Eqs. (7) and (6), the PDF of z_{\max} can be readily written as follows:

$$f_{z_{\max}}(z) = \sum_{u=1}^{|D|} (-1)^{u-1} \sum_{v=1}^{\binom{|D|}{u}} [\lambda_{uv} \exp(-\lambda_{uv} z)] \quad (8)$$

The outage probability is defined as the received SINR less than a given threshold value γ_{th} at MT.

$$P_{out} = \Pr(\gamma < \gamma_{th}) = 1 - \Pr(\gamma > \gamma_{th}) \quad (9)$$

With reference to [27,28], the right-hand part of Eq. (9) is given by:

$$\begin{aligned} & \Pr(\gamma > \gamma_{th}) \\ &= \Pr\left(\frac{z_{\max}}{L_{q,2} P_{q,2} |h_{q,2}|^2 + L_{l,3} P_{l,3} |h_{l,3}|^2 + \sigma_n^2 / S_s} > \gamma_{th}\right) \\ &= \sum_{u=1}^{|D|} (-1)^{u-1} \sum_{v=1}^{\binom{|D|}{u}} \exp\left(-\lambda_{uv} \gamma_{th} \sigma_n^2 / S_s\right) \times \\ & \quad \left(\frac{1}{\lambda_{uv} \gamma_{th} L_{q,2} P_{q,2} + 1} \frac{1}{\lambda_{uv} \gamma_{th} L_{l,3} P_{l,3} + 1}\right) \end{aligned} \quad (10)$$

The detailed derivation of Eq. (10) is given in Appendix A.

3.1 No shadowing scenario ($S_s = 1$)

The closed-form expression of outage probability at MT is given as:

$$P_{out}^{NS} = \Pr(\gamma < \gamma_{th}) = 1 - \Pr(\gamma > \gamma_{th})$$

$$= 1 - \sum_{u=1}^{|D|} (-1)^{u-1} \sum_{v=1}^{\binom{|D|}{u}} \exp\left(-\lambda_{uv}\gamma_{th}\sigma_n^2\right)$$

$$\left(\frac{1}{\lambda_{uv}\gamma_{th}L_{q,2}P_{q,2} + 1} \frac{1}{\lambda_{uv}\gamma_{th}L_{l,3}P_{l,3} + 1}\right) \quad (11)$$

3.2 Shadowing scenario

Taking shadowing effect into consideration, we can rewrite the outage probability as follows:

$$P_{out}^S = \int_0^\infty P_{out}^{NS} f_{S_s}(s) ds \quad (12)$$

It is hard to get the closed-form expression for Eq. (12), therefore, the Gauss-Hermite integral [25] is introduced to approximate, and the final result is given as:

$$P_{out}^S \simeq 1 - \frac{1}{\sqrt{\pi}} \sum_{u=1}^{|D|} (-1)^{u-1} \times$$

$$\sum_{v=1}^{\binom{|D|}{u}} \left(\frac{1}{\lambda_{uv}\gamma_{th}L_{q,2}P_{q,2} + 1} \frac{1}{\lambda_{uv}\gamma_{th}L_{l,3}P_{l,3} + 1}\right)$$

$$\times \sum_{w=1}^{N_w} H_w \exp\left(-\frac{\lambda_{uv}\gamma_{th}\sigma_n^2}{10(\sqrt{2}\sigma_{t_w} + \mu)/10}\right) \quad (13)$$

where t_w denotes the base point, H_w denotes the weight factor, and N_w is the order of the introduced Hermite polynomial (see also Appendix B).

In comparison with the results for the NCLT method, herein, the closed-form expression of outage probability with the CLT method is given. For CLT method, the interference plus noise is considered as constant when given propagation path-loss and transmitted power.

The SINR at MT is given by [13]:

$$\gamma_{CLT} = \frac{z_{\max}}{\delta_z^2} \quad (14)$$

where $\delta_z^2 = L_{q,2}P_{q,2} |h_{q,2}|^2 + L_{l,3}P_{l,3} |h_{l,3}|^2 + \sigma_n^2$.

Table 1 Simulation Parameters

Standard deviation of shadowing	$\sigma = 5_{\text{dB}}$
Mean of shadowing	$\mu = 0_{\text{dB}}$
Path exponent	$\alpha = 4.0$
Normalised radius for macro-cell	$R = 1$
Angle	$\theta = 0$
Threshold	$\gamma_{th} = 8.45_{\text{dB}}$
Hermite polynomial order	$N_w = 20$
Noise power	$\sigma_n^2 = 1$
Number of RAUs	$N = 7$

So, the PDF of γ_{CLT} is given as:

$$f_{\gamma_{CLT}} = \sum_{u=1}^{|D|} (-1)^{u-1} \sum_{v=1}^{\binom{|D|}{u}} \left[\frac{\lambda_{uv}}{\delta_z^2} \exp\left(-\frac{\lambda_{uv}\gamma}{\delta_z^2}\right)\right] \quad (15)$$

According to Eqs. (14–15), we can get the outage probability of MT as:

$$P_{out-CLT} = \Pr(\gamma < \gamma_{th})$$

$$= \sum_{u=1}^{|D|} (-1)^{u-1} \sum_{v=1}^{\binom{|D|}{u}} [1 - \exp(-\lambda_{uv}\gamma_{th})] \quad (16)$$

4 Simulation Results and Discussion

To verify the accuracy of the aforementioned analytical results, computer Monte-Carlo simulation is introduced in the following section. The distance between active MT and the objective cell centre is re-designated as d , which is normalised (i.e., $0 < d \leq 1$) for the convenience of analysis. It is assumed that in Cell-1 the moving route for MT-1 is from RAU-1 in the direction of θ to the cell edge, as shown in Figure 1. Furthermore, the reminder of simulation parameters are set as follows in Table 1.

Along the direction $\theta = 0^\circ$, the outage probability of SSTs in DAS versus the normalised distance d from the initial position (i.e., the objective cell centre) to the cell boundary, is depicted in Fig. 2. The analytical results by the NCLT method as well as the CLT method are clearly different, this is because the impact of short-term fading plays important role in the process of outage probability analysis. In comparison with NCLT method, interference plus noise is treated as a fixed-variance Gaussian noise when given propagation path-loss and transmitted power. The disadvantage of CLT method is that the impact of short-term fading is neglected. Therefore, it is more accurate to describe the outage probability with NCLT method.

Moreover, the outage probability of a DAS is higher than that of its surroundings when the MT is located at a cell

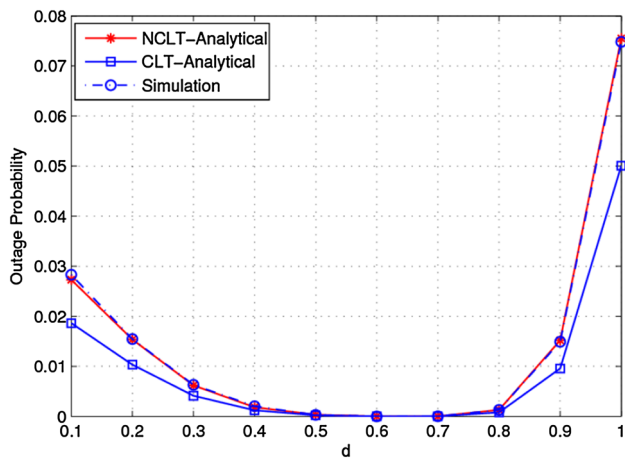


Fig. 2 Outage probability versus the normalised distance as $\theta = 0$ ($r = 0.65$)

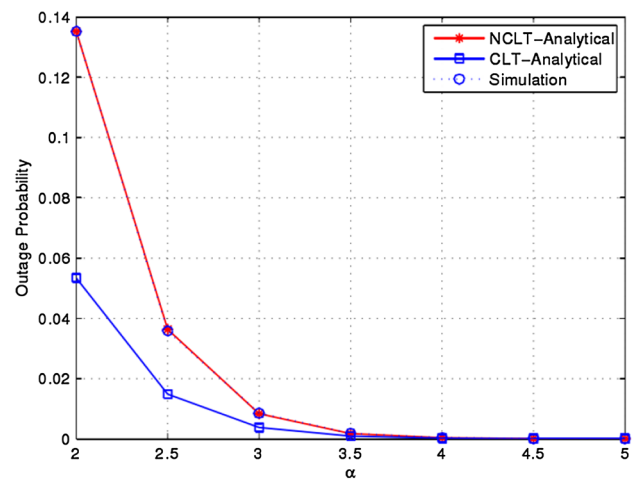


Fig. 4 Outage probability versus the path-loss exponent α as $r = 0.5$, $d = 0.65$

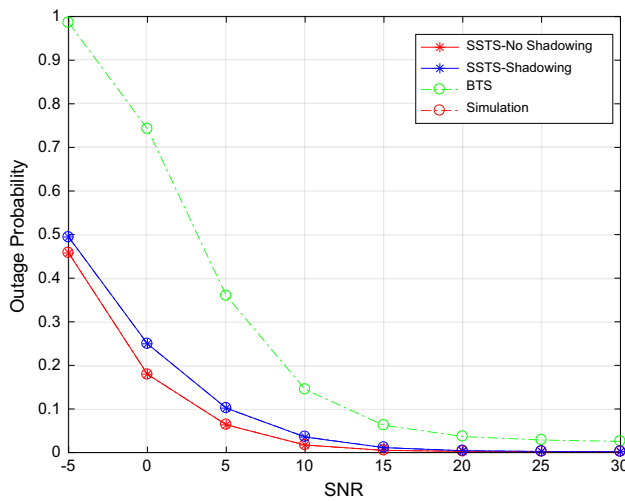


Fig. 3 Outage probability versus the signal-to-noise ratio as $\theta = 0$; $d = 0.9$ ($r = 0.65$)

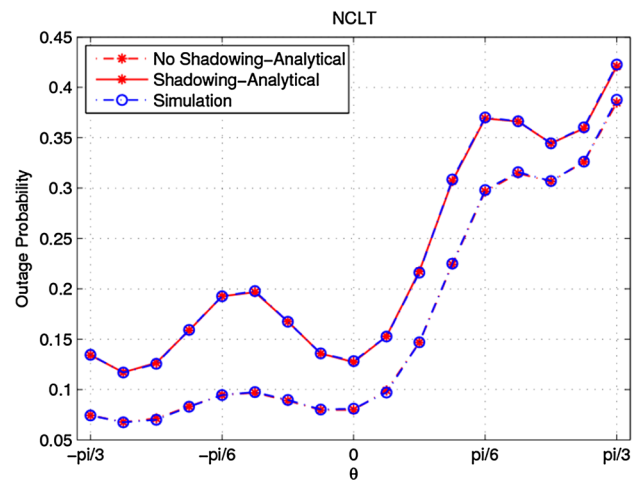


Fig. 5 Outage probability versus the angle θ as $r = 0.65$; $d = 1.0$ (NCLT)

centre as well as a cell edge, because the distance between MT and the selected RAU becomes greater. As the MT moves to the location of $d = 0.65$, the outage probability is lower, this is because the distance between the selected RAU and MT is nearer. It can be demonstrated from Fig. 2 that the theoretical analysis results throughout the paper is correct, this is because the simulation results and analytical results are in excellent agreement.

The outage probability of MT versus the signal-to-noise ratio (SNR) as $d = 0.9$, $\theta = 0$ is depicted in Fig. 3. It can be seen from Fig. 3 that the difference between no-shadowing and shadowing scenarios as well as between SSTS and BTS methods are obvious, this is because the shadowing fading has bad effect on the outage probability, which is the nature property of shadowing. Moreover, the outage probability of SSTS is better compared with BTS, this is because the advantage of selection diversity is embodied and the inter-cell

interferences reduce. It can also be demonstrated from Fig. 3 that the theoretical analysis results throughout the paper is correct, the explanation for this is the same as Fig. 2.

In the direction of $\theta = 0$, the outage probability versus path-loss exponent α is depicted in Fig. 4, as the position of MT is located at $d = 0.65$ together with $r = 0.5$. The outage probability performance decreases along with α increases, which is in conformity with the definition of propagation path-loss $L = d^{-\alpha}$. Therefore, the larger the value of α , the lower the propagation path-loss. It can be obtained from Fig. 4 that the outage probability of SSTS in DAS by NCLT method is more accurate than the counterpart by CLT method, because the impact of short-term fading on interference can be embodied. Moreover, it can be seen that the outage probability of SSTS in DAS outperforms the corresponding BTS scenario, the explanation for this is the same as Fig. 2.

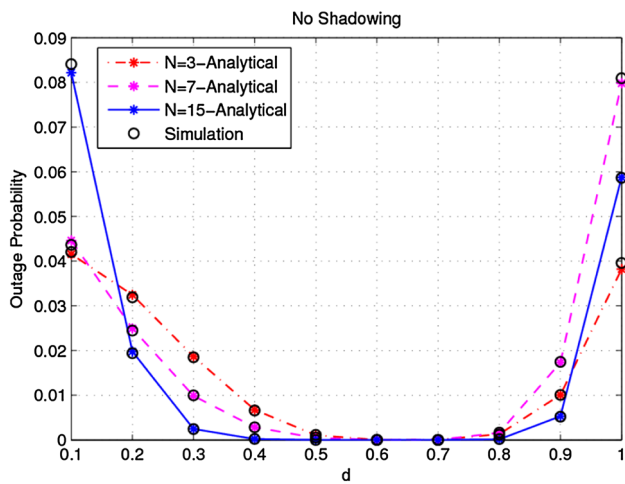


Fig. 6 Outage probability versus the normalised distance for different number of RAUs as $r = 0.65$ (NCLT)

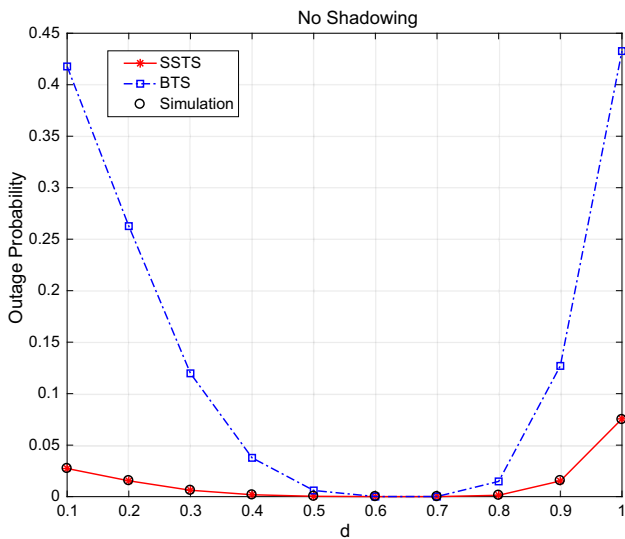


Fig. 7 Outage probability versus the normalised distance for SSTS and BTS at $r = 0.65$ (NCLT)

In Fig. 5, the outage probability *versus* θ for MT along the cell edge is plotted. The trends in SSTS and BTS are similar. There is a vertex around $\theta = -\pi/6$, because the RAU from Cell 3 is near the MT and has an effect on system performance. It is the same as vertex at $\theta = -\pi/6$. It has three valleys around $\theta = -\pi/4, 0, \pi/4$, respectively, because it exits from three RAUs in Cell 1 at the range $\theta \in (-\pi/3, \pi/3)$. As the MT moves, the RAU closest to the MT is selected. Therefore, the number of valleys matches the number of RAUs in the corresponding range. Moreover, it can be seen from Fig. 5 that shadowing fading has an adverse effect on outage probability, which is an shadowing’ innate property of itself.

The outage probability of SSTS in DAS *versus* the number of RAUs N is depicted in Fig. 6. It can be seen that the outage

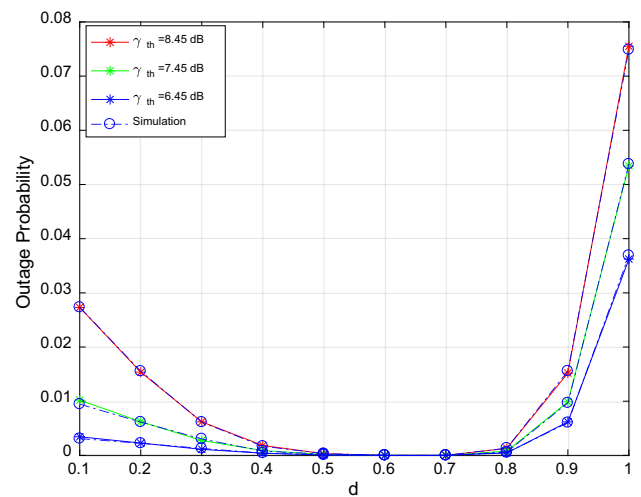


Fig. 8 Outage probability versus the normalised distance for SSTS at $r = 0.65$ (NCLT)

probability is lower than the surroundings when MT located at $d = 0.65$, because the RAU around $d = 0.65$ is chosen to transmit the signal with MT. Correspondingly, the communication distance between the selected RAU and MT becomes small, which can reduce outage probability. It also can be seen that the number of RAUs (N) has greatly influences on outage probability.

The outage probability of a DAS *versus* d with $r = 0.65$ is shown in Fig. 7. The whole transmitted power in each cell is the same for both SSTS and BTS in case of simulation. For SSTS, the outage probability is lower than that of BTS, this is because the reduced inter-cell interference and selection diversity play important roles. From Fig. 6, we see that, at the same outage probability, SSTS consumes less power than that of BTS. So, from the point of energy efficiency, SSTS offers better advantages compared to BTS.

The outage probability of DAS *versus* d as $r = 0.65$, $\theta = 0$ is illustrated in Fig. 8. The threshold values $\gamma_{th} = 6.45, 7.45, 8.45$ dB are selected as research object. With the values of threshold become large, the outage probability of DAS is worse, which is consistent with the definition of it.

5 Conclusions

In this paper, the interference power as well as its variance in DAS are considered as a random variable for the proposed NCLT method, when the propagation path-loss and transmitted power are given. For the proposed NCLT method, the effect of short-term fading on interference plus noise can be embodied, which can describe the outage probability more accurately. So this proposed NCLT method is more practical and accurate to evaluate the system performance of DAS. Moreover, an SSTS for DAS is proposed on the basis of the

maximum desired signal criterion. Downlink outage probability of DAS for the proposed SSTS is investigated and the closed-form expressions of it are derived under no shadowing conditions, while the corresponding approximate analytical expressions for shadowing conditions are also given. Finally, it can be concluded that the proposed NCLT method is more accurate to describe outage probability when compared with CLT method. In the near future, many interesting issues on basis of this work are worth further investigation. Orthogonal frequency-division multiple access (OFDMA) as an important interference cancellation technology can be introduced to improve the system performance of DAS. Nakagami-m fading channel is more general in practice, and the closed-expression for DAS can be derived when channels suffer from this fading. Hence, it is meaningful to investigate the application of OFDMA and Nakagami-m fading to DAS in future work.

Appendix A: derivation of Eq. (10)

$$\begin{aligned}
 & \Pr(\gamma > \gamma_{th}) \\
 &= \Delta \Pr\left(\frac{z_{\max}}{L_{q,2}P_{q,2}|h_{q,2}|^2 + L_{l,3}P_{l,3}|h_{l,3}|^2 + \sigma_n^2/S_s} > \gamma_{th}\right) \\
 &= \int_{t_2=0}^{\infty} \int_{t_3=0}^{\infty} \Pr(z_{\max} > \gamma_{th}(t_2 + t_3 + \sigma_n^2/S_s)) \\
 &\times \exp\left(\frac{-t_2}{L_{q,2}P_{q,2}}\right) \exp\left(\frac{-t_3}{L_{l,3}P_{l,3}}\right) dt_2 dt_3 \\
 &= \Delta \sum_{u=1}^{|D|} (-1)^{u-1} \sum_{u=1}^{\binom{|D|}{u}} \int_{t_2=0}^{\infty} \int_{t_3=0}^{\infty} \exp(-\lambda_{uv}\gamma_{th} \\
 &\quad (t_2 + t_3 + \sigma_n^2/S_s)) \\
 &\times \exp\left(\frac{-t_2}{L_{q,2}P_{q,2}}\right) \exp\left(\frac{-t_3}{L_{l,3}P_{l,3}}\right) dt_2 dt_3 \\
 &= \Delta \sum_{u=1}^{|D|} (-1)^{u-1} \\
 &\times \sum_{u=1}^{\binom{|D|}{u}} \exp(-\lambda_{uv}\gamma_{th}\sigma_n^2/S_s) \\
 &\int_{t_2=0}^{\infty} \int_{t_3=0}^{\infty} \exp\left(\frac{-\lambda_{uv}\gamma_{th}L_{q,2}P_{q,2} - 1}{L_{q,2}P_{q,2}}\right) \\
 &\times \exp\left(\frac{-\lambda_{uv}\gamma_{th}L_{l,3}P_{l,3} - 1}{L_{l,3}P_{l,3}}\right) dt_2 dt_3 \\
 &= \Delta \sum_{u=1}^{|D|} (-1)^{u-1} \sum_{u=1}^{\binom{|D|}{u}} \exp(-\lambda_{uv}\gamma_{th}\sigma_n^2/S_s) \\
 &\times \left[\frac{L_{q,2}P_{q,2}}{\lambda_{uv}\gamma_{th}L_{q,2}P_{q,2} + 1} \frac{L_{l,3}P_{l,3}}{\lambda_{uv}\gamma_{th}L_{l,3}P_{l,3} + 1}\right]
 \end{aligned}$$

$$\begin{aligned}
 &= \Delta \sum_{u=1}^{|D|} (-1)^{u-1} \sum_{u=1}^{\binom{|D|}{u}} \exp(-\lambda_{uv}\gamma_{th}\sigma_n^2/S_s) \\
 &\left(\frac{1}{\lambda_{uv}\gamma_{th}L_{q,2}P_{q,2} + 1} \frac{1}{\lambda_{uv}\gamma_{th}L_{l,3}P_{l,3} + 1}\right) \tag{17}
 \end{aligned}$$

where $\Delta = \frac{1}{L_{q,2}P_{q,2}} \frac{1}{L_{l,3}P_{l,3}}$

Appendix B: Gauss-Hermite quadrature

The Gauss-Hermite formula is expressed as [29]:

$$\begin{aligned}
 \int_{-\infty}^{+\infty} \exp(-x^2) f(x) dx &= \sum_{i=1}^n H_i f(x_i) + R_n \\
 &\simeq \sum_{i=1}^n H_i f(x_i) \tag{18}
 \end{aligned}$$

where n is the order of Hermite polynomial (the number of sample points utilized for the approximation). The value x_i is the roots of the Hermite polynomial $H_n(x)$ ($i = 1, \dots, n$) and the associated weights H_i are given as:

$$H_i = \frac{2^{n-1} n! \sqrt{\pi}}{n^2 [H_{n-1}(x_i)]^2} \tag{19}$$

The Hermite polynomial $H_n(x)$ is written as [28]:

$$\begin{aligned}
 H_n(x) &= (-1)^n \exp(x^2) \frac{d^n}{dx^n} (\exp(-x^2)) \text{ or} \\
 H_n(x) &= 2^n x^n - 2^{n-1} \binom{n}{2} x^{n-1} + \\
 &2^{n-2} \cdot 1 \cdot 3 \cdot \binom{n}{4} x^{n-4} - 2^{n-3} \cdot 1 \cdot 3 \cdot 5 \cdot \binom{n}{6} x^{n-6} + \dots \\
 H_0(x) &= 1 \tag{20}
 \end{aligned}$$

The remainder in Eq. (15) is given as:

$$R_n = \frac{n! \sqrt{\pi}}{2^n (2n)!} f^{(2n)}(\xi) \quad (-\infty < \xi < \infty) \tag{21}$$

where ξ is arbitrarily chosen and $f^{(n)}(x)$ is the n^{th} derivative of $f(x)$.

The precision of the Gauss-Hermite approximation is dominated by n . If the number of sample points (n) is insufficient, the approximate and exact curves do not match exactly. On the contrary, the larger n , the more accurate the approximation obtained.

References

1. Kim, H., Lee, S.R., Song, C., Lee, K.J., Lee, I.: Optimal power allocation scheme for energy efficiency maximization in distributed antenna systems. *IEEE Transact. Commun.* **63**(2), 431–440 (2015)
2. Heath, R., Peters, S., Wang, Y., Zhang, J.: A current perspective on distributed antenna systems for the downlink of cellular systems. *IEEE Commun. Mag.* **51**(4), 161–167 (2013)
3. Feng, W., Ge, N., Lu, J.: Hierarchical transmission optimization for massively dense distributed antenna systems. *IEEE Commun. Lett.* **19**(4), 673–676 (2015)
4. You, X.H., Wang, D.M., Sheng, B., Gao, X.Q., Zhao, X.S.: Cooperative distributed antenna systems for mobile communications [coordinated and distributed MIMO]. *IEEE Wireless Commun.* **17**, 35–43 (2010)
5. Lee, S.-R., Moon, S.-H., Kong, H.-B., Lee, I.: Optimal beamforming schemes and its capacity behavior for downlink distributed antenna systems. *IEEE Trans. Wireless Commun.* **12**(6), 2578–2587 (2013)
6. Ren, H., Liu, N., Pan, C., He, C.: Energy efficiency optimization for mimo distributed antenna systems. *IEEE Transact. Veh. Technol.* **66**(3), 2276–2288 (2017)
7. Saleh, A., Rustako, A.J., Roman, R.S.: Distributed antennas for indoor radio communications. *IEEE Trans. Commun.* **35**(12), 1245–1251 (1987)
8. Choi, W., Andrews, J.G.: Downlink performance and capacity of distributed antenna systems in a multicell environment. *IEEE Trans. Wireless Commun.* **6**(1), 69–73 (2007)
9. Zhou, S., Zhao, M., Xu, X., Wang, J.: Distributed wireless communication systems: a new architecture for future public wireless access. *IEEE Commun. Mag.* **41**(3), 108–113 (2003)
10. Zhu, H.L.: Performance comparison between distributed antenna and microcellular systems. *IEEE J. Sel. Areas Commun.* **29**(6), 1151–1163 (2011)
11. Nosratinia, A., Hunter, T.E., Hedayat, A.: Cooperative communication in wireless networks. *IEEE Commun. Mag.* **42**(10), 74–80 (2004)
12. Katranaras, E., Imran, M.A., Tzaras, C.: Uplink capacity of a variable density cellular system with multicell processing. *IEEE Trans. Commun.* **57**(7), 2098–2108 (2009)
13. You, X., Wang, D., Zhu, P., Sheng, B.: Cell edge performance of cellular mobile systems. *IEEE J. Sel. Areas Commun.* **29**(6), 1139–1150 (2011)
14. Park, J., Song, E., Sung, W.: Capacity analysis for distributed antenna systems using cooperative transmission schemes in fading channels. *IEEE Trans. Wireless Commun.* **8**(2), 586–592 (2009)
15. Liu, Y.X., Liu, J., Chen, H., Zheng, L.N., Zhang, G.W., Guo, W.D.: Downlink performance of distributed antenna systems in multicell environment. *IET Commun.* **5**(15), 2141–2148 (2011)
16. Choi, W., Andrews, J.G.: Theoretical limits of cellular systems with distributed antennas. In: Hu, H.L., Zhang, Y., Luo, J.J. (eds.) *Distributed Antenna Systems: Open Architecture for Future Wireless Communications*, pp. 65–86. Auerbach Press, Berlin (2007)
17. Vereecken, W., Heddeghem, W.V., Deruyck, M., Puype, B., Lannoo, B., Joseph, W., Colle, D., Martens, L., Demeester, P.: Power consumption in telecommunication networks: overview and reduction strategies. *IEEE Commun. Mag.* **49**(3), 62–69 (2011)
18. Liu, Y.X., Liu, J., Guo, W.D., Chen, H., Zheng, D., Zhang, G.W.: Downlink performance analysis of distributed antenna systems. In: *Proceedings of the IEEE International Conference on Wireless Communication and Signal Processing*, pp. 1–5. Nanjing (2011)
19. Liu, Y.X., Chen, P., Ouyang, H., Fang, H.W.: Bit error rate of SSTS for downlink distributed antenna systems in multicell environment. *Wireless Pers. Commun.* **31**(3), 1063–1078 (2015)
20. Wyner, A.: Shannon-theoretic approach to a Gaussian cellular multiple-access channel. *IEEE Trans. Inf. Theory* **40**(6), 1713–1727 (1994)
21. Zhang, H., Dai, L., Xiao, L., Yao, Y.: Spectral efficiency of distributed antenna system with random antenna layout. *Electron. Lett.* **39**(6), 495–496 (2003)
22. Wang, X., Zhu, P., Chen, M.: Antenna location design for generalized distributed antenna systems. *IEEE Commun. Lett.* **13**(5), 315–317 (2009)
23. Zhang T., Zhang C., Cuthbert L., Chen Y.: Energy efficient antenna deployment design scheme in distributed antenna systems. In: *Proceedings of the IEEE International 72nd Vehicular Technology Conference*, pp. 1–5. Spring (VTC 2010-Fall), Ottawa, (2010)
24. Zhang W., Diao C., Zhao M., Chen M.: Impact of path loss exponents on antenna location design for GDAS. In: *Proceedings of the IEEE International 75nd Vehicular Technology Conference*, pp. 1–5. Spring VTC 2012-Spring, Yokohama (2012)
25. Chen, H.M., Wang, J.B., Chen, M.: Outage performance of distributed antenna systems over shadowed Nakagami-m fading channels. *Eur. Trans. Telecommun.* **20**(5), 531–535 (2009)
26. Chen, H., Liu, J., Zheng, L.N., Zhai, C., Zhou, Y.: Approximate SEP analysis for DF cooperative networks with opportunistic relaying. *IEEE Signal Process. Lett.* **17**(9), 777–780 (2010)
27. Simon, M.K., Alouini, M.S.: *Digital Communication Over Fading Channels: A Unified Approach to Performance Analysis*, pp. 99–140. Wiley, New Jersey (2000)
28. Gradshteyn, I., Ryzhik, I.: *Table of Integrals, Series, and Products*. Academic Press, New York (2003)
29. Abramowitz, M., Stegun, I.A.: *Handbook of Mathematical Functions with Formulas, Graphs, and Mathematical Tables*. Dover Publications, New York (1970)



Sitong Lv was born in Jilin Province, China, in 1983. She received her B.S. degree in Electronic and Information from Yantai University (YTU), Yantai, China, in 2006, and M.S. degree in communication engineering from Jilin University (JLU), Jilin, China, in 2008. She's currently pursuing a Ph.D. degree in engineering at Jilin University (JLU), Jilin, China. Since September 2008, she has been working at the Aviation University of AirForce, Jilin, China. Her

research interests include distributed antenna system, cooperative communications, multi-input multi-output and internet of things (IOT).



Zhihong Qian was born in Jilin Province, China, in 1957. He is a professor, doctoral tutor of Communication Engineering Institute of JiLin University in Changchun, China. Senior Member of IEEE. The principal person in charge of Wireless Network Laboratory of JiLin university. His main research direction is the area of Internet of Things and wireless network.



Yuxi Liu was born in Shandong Province, China, in 1984. He received his B.S. degree in Electronic and Information from Yantai University (YTU), Yantai, China, in 2006, and M.S. degree in signal processing from Nanjing University of Science and Technology (NJUST), Nanjing, China, in 2008. He received his Ph.D. degree in Communication and Information System from Shandong University (SDU), Jinan, China, in 2012.

Since July 2012, he has been with the State Grid Information and Telecommunication Group Co., Ltd. His research interests include distributed antenna system, cooperative communications, multi-input multi-output, femtocell, power line communications (PLC), and smart grid.